Thermochimica Acta, 38 (1980) 211—223

AN AUTOMATED TECHNIQUE FOR THERMOACOUSTIMETRY OF SOLIDS *

T. MRAZ, K. RAJESHWAR ** and J. DUBOW

Department of Electrical Engineering, Colorado State University, Fort Collins, CO 80523 (U.S.A.)

(Received 13 November 1979)

ABSTRACT

An automated technique for thermoacoustimetry of solids is described. The technique is illustrated by measurements on Green River and Kentucky oil shales.

INTRODUCTION

Conventional thermal analysis techniques such as differential scanning calorimety (DSC) and thermogravimetry (TG) yield information which usually reflects only the gross macroscopic thermal behavior of the test material. The sensitivity of these techniques can, however, be magnified by combining them with probes which are responsive to changes taking place in the sample on a molecular level. In a previous paper, a classification scheme was proposed wherein primary thermal analysis techniques (e.g., DSC, TG) comprised one group (Group A), and techniques which yield mechanistic information fell under the second group (Group B) [1]. An ideal combination of thermal analysis experiments was then defined as that coupling techniques in Group A with methods listed under Group B [1]. Amongst the techniques that would fall under the latter category (Group B), mention may be made of thermoelectrometry [1,2], thermosonimetry [3], thermophotometry [4], mass spectrometry [5—7], and thermoacoustimetry [8]. In this paper, we describe an automated technique for thermoacoustimetric measurements on solids. The technique is illustrated by measurements on oil shale samples from eastern and western United States.

The Nomenclature Committee of the International Confederation on Thermal Analysis (ICTA) recommends the following definition for thermoacoustimetry: "A technique in which the characteristics of imposed acoustic waves are measured as a function of temperature after passing through a substance while the substance is subjected to a controlled temperature program" [9]. A closely related technique is that of thermosonimetry [3], wherein the

---

* Paper presented at the 9th NATAS Conference, Chicago, IL, 23—26 September 1979.
** To whom correspondence should be addressed.

sonic waves emitted by a substance are monitored as a function of temperature.

A variety of techniques exist for measuring the characteristics (e.g., velocity, attenuation) of sound waves in solids. A considerable volume of work is cited in the geophysical literature [10—14]. The various techniques for the measurement of attenuation and velocities of shear (S) and compressional (P) waves have been reviewed recently [15,16]. Essentially, these techniques differ only in the nature of sample support and transducer geometry which is employed. The technique to be described in this paper incorporates many of the details employed by previous authors plus some unique features which permit automatic acquisition of data while the sample is being subjected to a controlled temperature program. Both S and P wave velocities can be measured in a single experiment as a function of temperature and chosen variables such as atmosphere, confining pressure, etc. The sample holder arrangement to be described is also readily amenable to coupling with DSC or differential thermal analysis (DTA).

EXPERIMENTAL

The techniques described in the literature for measurement of acoustic velocities can be classified into two broad categories:

(a) those which are based on the determination of ultrasonic frequencies at which continuous sinusoidal waves propagate repetitively across the sample with constructive interference [17]. This group also comprises variants of this method including the pulse-echo-overlap technique [18], ultrasonic interferometry [19] and resonance-frequency technique; and

(b) techniques involving precise measurement of transmission times of S and P waves across a sample of known dimensions. The majority of techniques in the latter group employ the detection of first-arrival times and usually involve two transducers (a sender and a receiver) in contact with the sample surface. The technique to be described in this paper belongs to this category. A pair of lithium niobate ($LiNbO_3$) transducers contact the opposite faces of the test sample — one to induce the incident acoustic signal and the other to detect the transmitted signal. A block diagram of the test set-up is shown in Fig. 1. Pertinent features of the various components of the test set-up and their relevance to the measurement procedure are amplified in the following paragraphs.

Sample holder

Figure 2 illustrates the sample holder arrangement which was employed for thermoacoustimetry. The stack assembly is not drawn to scale — the actual assembly measures ~53 cm from the base-plate to the top support bar. The base-plate is built up from a 25.4 cm square of 2.5 cm thick aluminum sheet. The top and bottom cooling blocks are made of aluminum with built-in water-cooled coils to prevent excessive conduction of heat to the piston assembly and base-plate. The asbestos insulator blocks, ~4 cm thick,

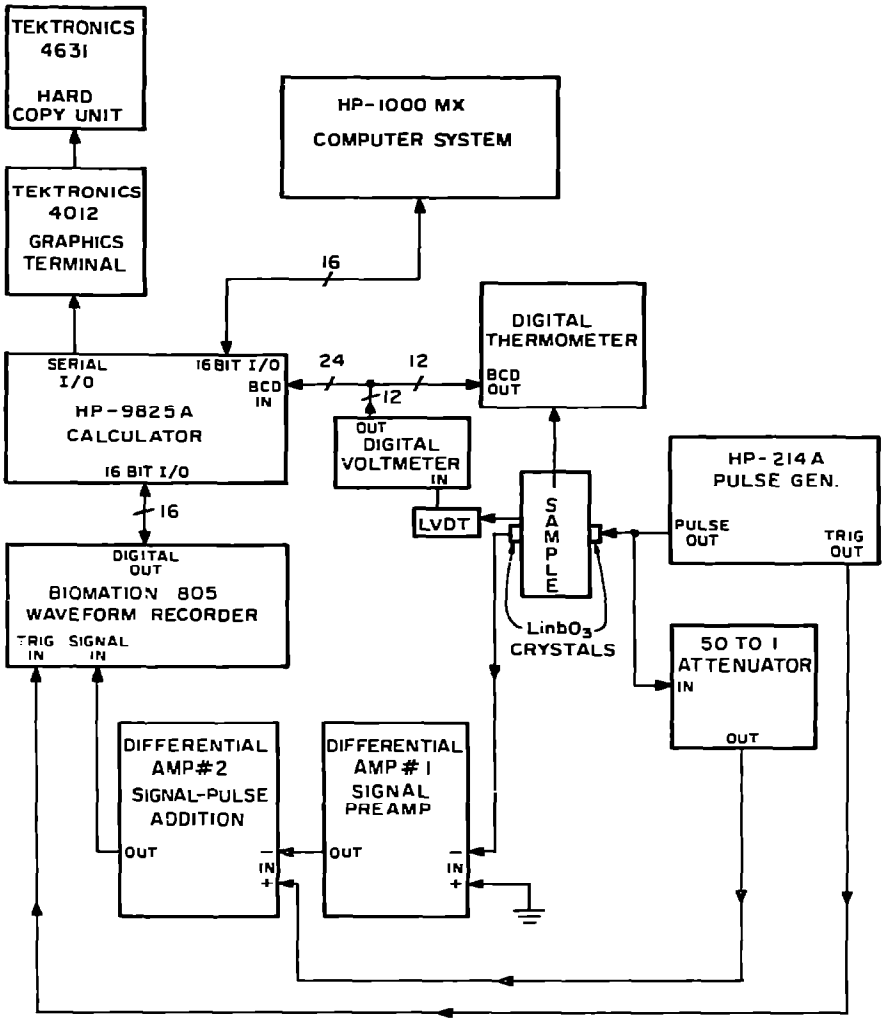

Fig. 1. Schematic of measurement set-up for thermoacoustimetry.

provide support for the heater assembly. The top and bottom stainless steel heater blocks contain nichrome-wound ceramic inserts and are driven by matched temperature programmers. The aluminum spacers sandwich the ceramic disks and the test sample and are necessary to provide electrical shielding for noise reduction. They also serve to minimize thermal gradients across the test sample. The ceramic disks, which hold the sample and transducers together, are 7.6 cm in diameter and 2.5 cm thick. Sample dimensions that can be accommodated in the test stack are rather flexible, and samples could range in length from ~1.8 cm to 7.6 cm and in diameter from 2.5 cm to 5.0 cm. Electrical contact to the transducers is provided by thin silver plates at the top and small aluminum electrodes embedded in the ceramic disks as shown in Fig. 2. The silver plates also help excessive noise arising from electric field-coupling between the driver and receiver transducers.

The entire stack assembly is held together under pressure exerted by a piston, which is pressurized from a nitrogen storage tank through a variable

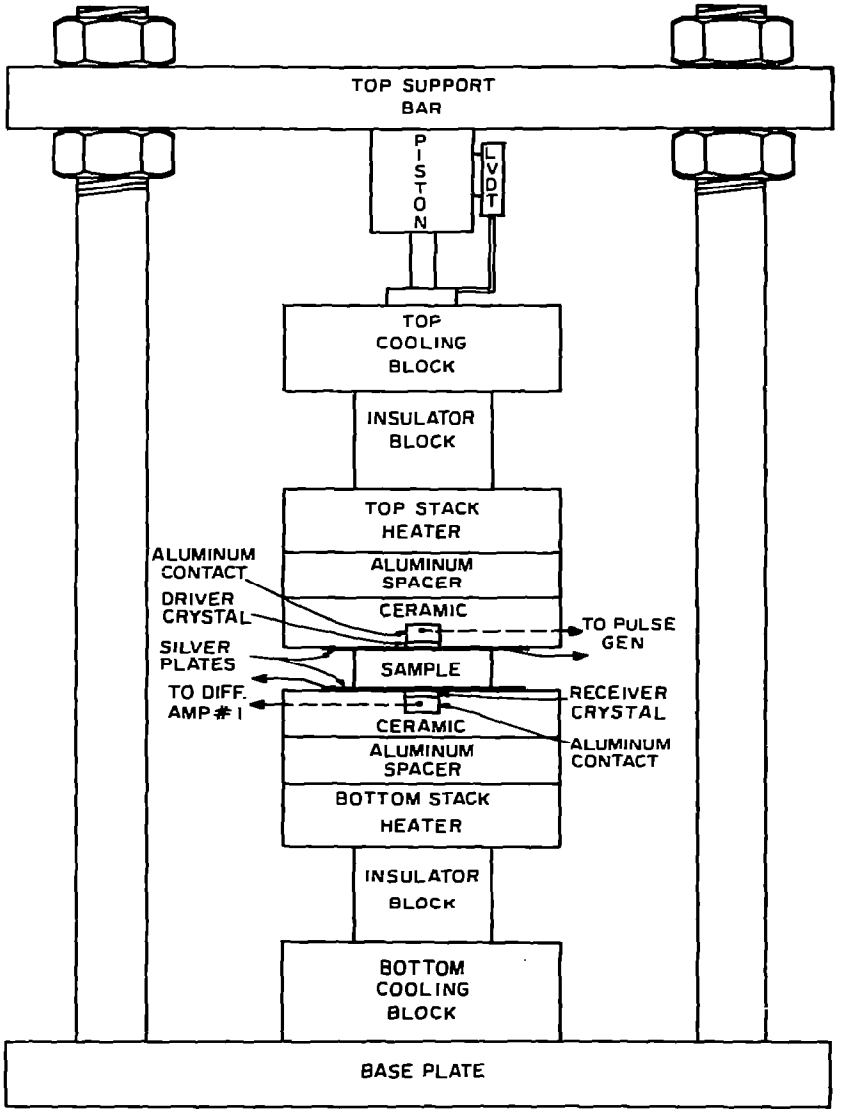

Fig. 2. Sample holder arrangement for thermoacoustimetry.

pressure check valve (not shown in Fig. 2). The confining pressure (~3 atm) is sufficient to maintain good mechanical coupling between transducer and test sample so that no bonding agent is necessary. The pressure on the sample is also kept constant throughout the experiment. Any excess pressure developed by thermal expansion of the test sample is released through the check valve. The sample expansion is also continuously monitored on the linear voltage differential transformer (LVDT) so that changes in sample dimensions may be taken into account for computation of S and P velocities (see below).

An aluminum bell jar (not shown in Fig. 2) encases the entire assembly and serves to control the atmosphere surrounding the test samples. A flowing atmosphere of dry, pre-purified N_2 is usually employed for the measurements described in this paper. This sweep-gas prevents spurious effects arising

from sample oxidation and also avoids self-generated atmospheres by removing any gases evolved during thermal decomposition of the test sample.

Transducers

41°-X cut $LiNbO_3$ crystals, approximately 0.6 cm diameter and 0.06 cm thick, were used to induce and detect acoustic waves in the sample. Lithium niobate was chosen because of its good piezoelectric response at high temperatures and the 41°-X orientation was used to allow detection of both P and S waves by the same crystal [20].

Instrumentation

The input pulse is generated by a HP-214A pulse generator (see Fig. 1). This 50 V, 100 μsec duration square wave, when applied to the driving transducer, causes an acoustic wave to propagate through the sample. The pulse rate is chosen to be as rapid as possible but slow enough to allow damping of an initial wave train before application of the next pulse. The transmitted signal from the receiver transducer is inverted and amplified by differential amplifier No. 1 (Fig. 1). This amplifier has a lower 3dB frequency of 10 kHz, an upper 3dB frequency of 0.1 MHz and a gain of 10 k to 50 k depending on the input pulse amplitude. The narrow frequency range employed for this amplifier provides adequate signal amplification without significant loss of information content, as well as good noise rejection which is important for the low signal levels encountered in the experiment.

An attenuated version of the driving pulse is then added to the output from amplifier No. 1 by amplifier No. 2 (Fig. 2). A much wider frequency response of DC to 1 MHz is used for this amplifier to keep the pulse rise-time as sharp as possible, and the gain is usually unity. This summation procedure is a unique feature of the present technique and enables detection of P and S wave first-arrival times as well as the instant of triggering of the input pulse, all on the same waveform. The output from amplifier No. 2 is fed into a Biomation Corporation Model 805 Waveform Recorder for digitization and subsequently transferred to a Hewlett Packard Model 9825A desk-top calculator. The latter also provides on-line control of the entire experiment. Data are recorded only at a desired time or temperature when the calculator arms the waveform recorder. When armed, a pre-trigger from the pulse generator enables the recorder to start data sampling at a point just prior to the rising edge of the pulse. The signal is sampled every 0.2 μsec with the eight-bit digital representation being stored in the recorder memory. After the recorder memory is saturated with 2048 sample points, the first 500 data points of the signal, where all the useful information is contained, are transferred to the calculator system. Once in the calculator memory, the data can be plotted either on a Tektronics Corporation Model 4012 Graphics System or transferred to the Hewlett Packard MX 1000 computer for storage and further analysis. A typical waveform on display in the graphics terminal is shown in Fig. 3.

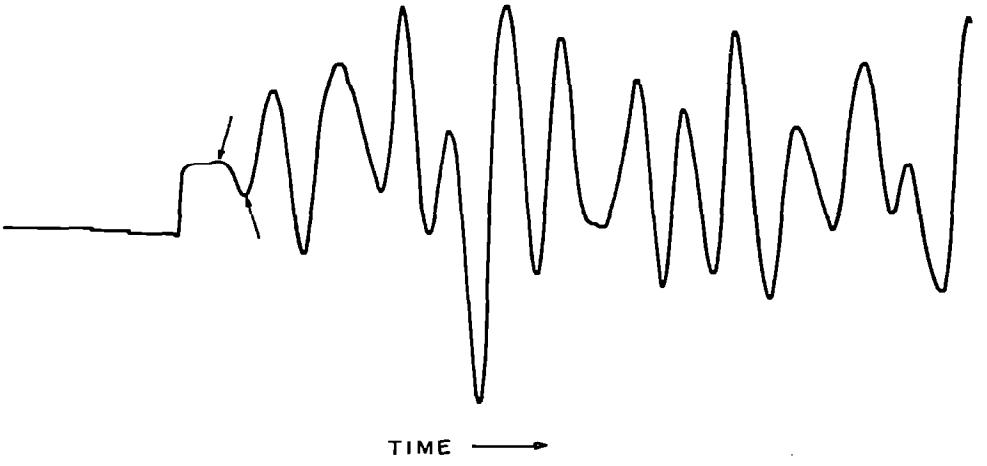

Fig. 3. Typical waveform observed for the transmitted acoustic signal.

Data analysis

A flowchart of the procedure employed for an acoustic velocity measurement is illustrated in Fig. 4. Information on sample length and density is entered into the computer program prior to the experiment. Changes in sample length as a function of temperature are automatically calculated from the voltage output of the LVDT. No correction was made for changes in sample density as a function of temperature in the present study although such corrections may be easily incorporated in the software package for the experiment.

The raw experimental data are usually stored in floppy disk memory in the computer system. Reduction of these data to P and S wave velocities, V_P and V_S, respectively, is performed by a slope variation detection algorithm developed in this laboratory [21]. The essence of this algorithm lies in the detection of a drastic change in slope on arrival of the P wave (shown by the first arrow in Fig. 3) and an upward deflection on subsequent arrival of a shear (S) wave (second arrow in Fig. 3). Each scan taken at increasing temperature intervals is superimposed on the preceding wave pattern and the curves are shifted back in time in increments of one unit (0.2 μsec). The algorithm then compares an interval of ±15 points about the known P or S wave arrivals with the preceding low temperature curve to see how closely the two patterns match after shifting. This procedure is repeated until the difference between the two curves is minimized. This increment is then added to the P or S wave arrival times in the preceding scan to obtain a window (±10 points) where the P or S wave is most likely to be found. The slope is computed from one point to the next within this window. A sudden change in slope corresponds to the arrival time of the P or S wave. The P or S wave transit time is then computed from the number of increments between the initial pulse and the first P wave arrival, $\Delta_1 t_P$ and the number of increments between the pulse rise and the first S wave arrival, $\Delta_2 t_s$

$$\Delta t_P = (\Delta_1 t_P \times 0.2)\ \mu\text{sec}$$
$$\Delta t_S = (\Delta_2 t_S \times 0.2)\ \mu\text{sec} \qquad (1)$$

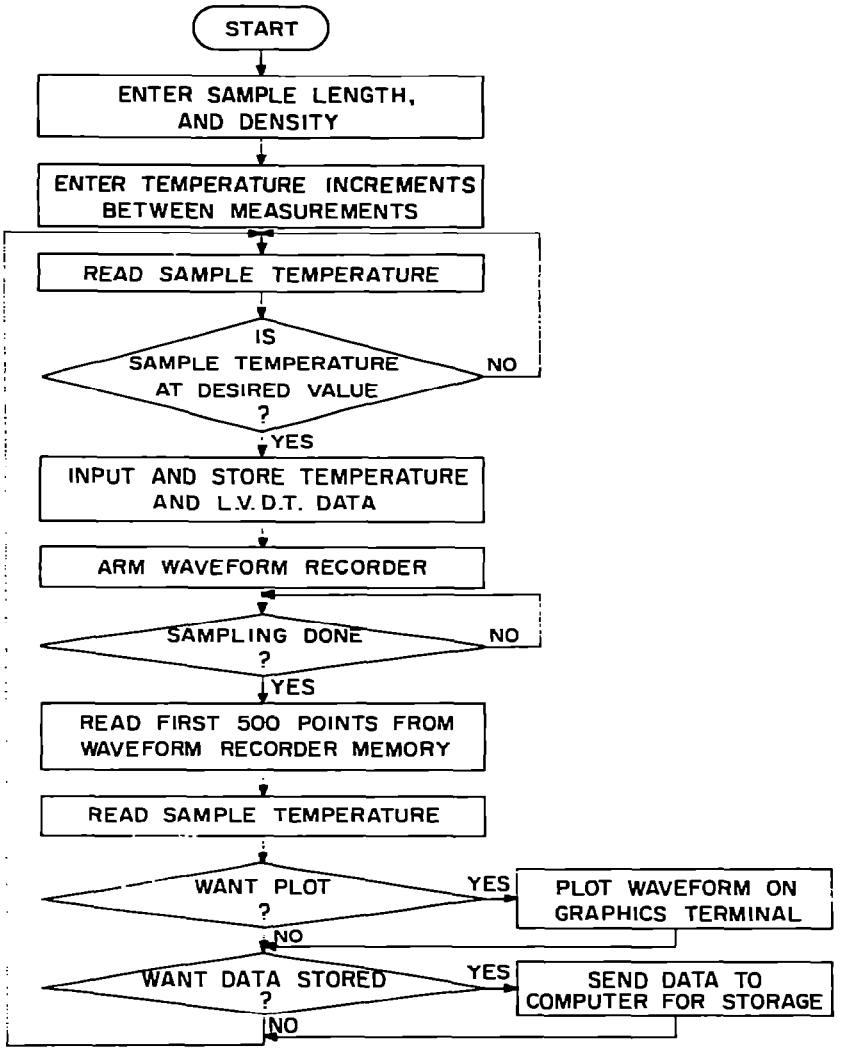

Fig. 4. Flow chart of procedure employed for measurement of acoustic velocities.

The 0.2 μsec interval employed for successive data sampling points results in a limiting resolution of the same value for the computed transit times.

Compressional or shear wave velocities, V_P and V_S can be calculated from the corresponding transit times and the sample length at any given temperature. Once V_P and V_S are known, the various elastic moduli can be calculated for the test material of known density from the following equations [22]

$$E = 2\rho V_S^2(1 + \upsilon) \tag{2}$$

$$G = \rho V_S^2 \tag{3}$$

$$B = \rho V_P^2 - 4/3\rho V_S^2 \tag{4}$$

$$\upsilon = \frac{V_P^2 - 2V_S^2}{2(V_P^2 - V_S^2)} \tag{5}$$

where E = Young's Modulus, G = shear modulus, B = bulk modulus, υ = Poisson's ratio and ρ = sample density. It is pertinent to note that these equations are valid only when the test material exhibits elastic behavior.

Calibration

Delay times associated with various parts of the test assembly (e.g., transducers) were characterized by measurements on calibration standards with accurately known P and S wave velocities. A machined aluminum rod (6.03 cm length and 5 cm diameter) was employed for this purpose. Values of V_S and V_P for this material were taken from a previous study [23]. The instrument delay time computed from the measured transit times and reported velocities were incorporated in the software package described above and corrections applied to the corresponding data points at each temperature for the test sample.

Samples

Samples of Green River oil shale were obtained from the U.S. Department of Energy Mine at Anvil Points near Rifle, Colorado. Kentucky oil shale samples were obtained from the Sweetland Creek member of the New Albany deposits. Other relevant details of sample preparation may be found in previous papers from this laboratory [24,25].

RESULTS AND DISCUSSION

Figure 5 shows the dependence of P wave velocities on temperature for Green River oil shales. Shale grade * is shown as the variable parameter. A regular decrease in acoustic velocities with both increasing temperature and increasing organic content is evident. Figure 6 illustrates the corresponding data on S wave velocities. As in the previous case, a decrease in velocity with increasing temperature and shale grade is characteristic of all the shale samples that were examined. A detailed discussion of the thermomechanical behavior of oil shales is beyond the scope of this article. It is, however, pertinent to note the good sensitivity of acoustic properties to the amount of organic matter in the shale (Figs. 5 and 6). Figures 7 and 8 illustrate the degree of reproductivity that is usually obtained for the measured P and S wave velocities, respectively. The data are shown for samples of Kentucky oil shale assaying about 13 gallons per ton (gpt). The two curves in each figure refer to measurements on two separate samples. Even better reproducibility than that seen in Figs. 7 and 8 would be expected for "pure" materials, i.e., materials that are more homogeneous than oil shales in general.

* Shale grade herein refers to the organic content of the shale and is expressed in terms of a Fischer assay equivalent which yields the volume of liquid fuel that can be extracted per unit mass of shale.

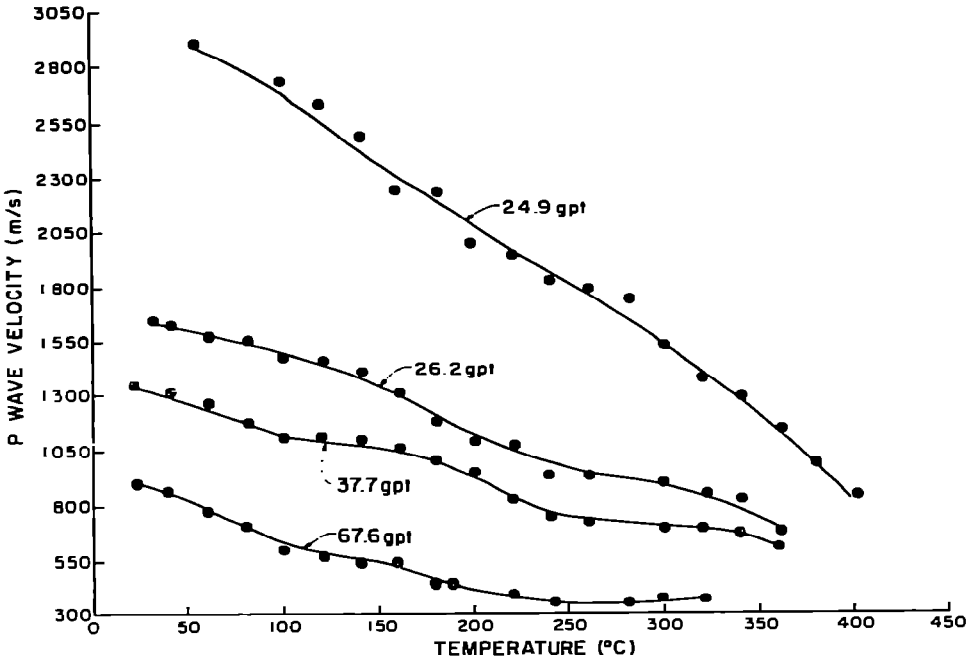

Fig. 5. Dependence of compressional (P) wave velocity on temperature for Green River oil shales. Shale grade is shown as the variable parameter (see text).

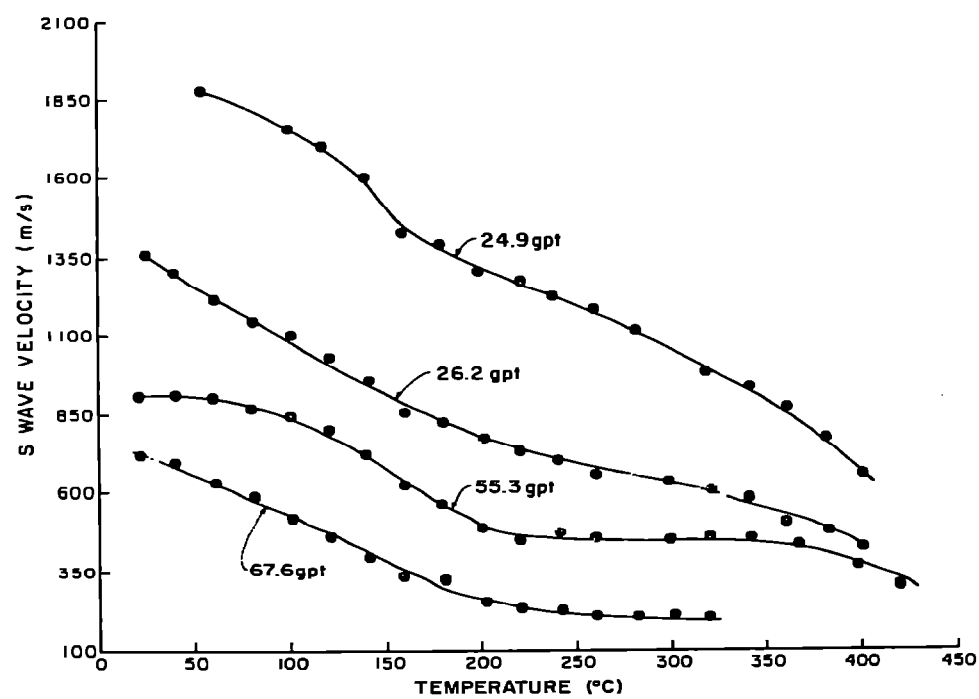

Fig. 6. Dependence of shear (S) wave velocity on temperature for Green River oil shales. Shale grade is shown as the variable parameter (see text).

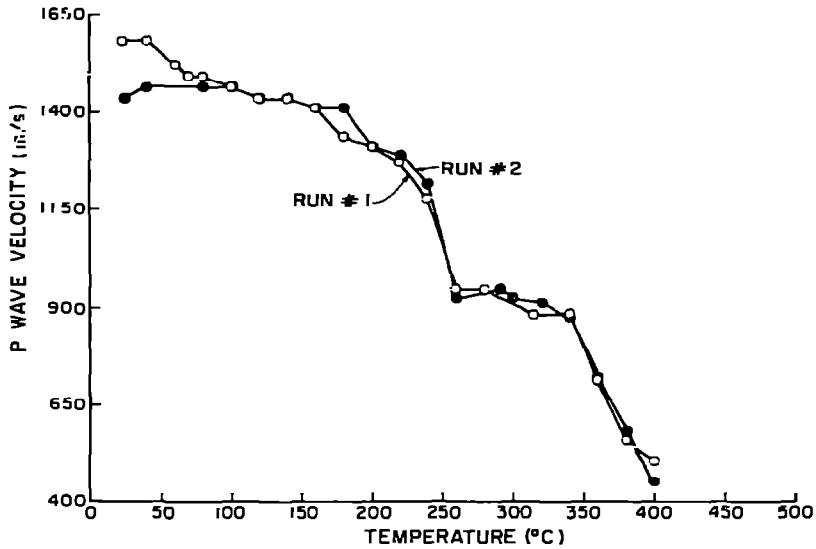

Fig. 7. Dependence of P wave velocity on temperature for a Kentucky oil shale sample. Runs 1 and 2 represent duplicate experiments.

Figure 9 shows the dependence of Young's modulus on temperature for Green River oil shales. Shale grade is again shown as the variable parameter. Figure 10 shows the corresponding data on the shear modulus. These values were calculated from the corresponding P and S wave velocities using eqns. (2) and (3). The same broad trends are observed as in Figs. 5 and 6.

The discontinuities and peaks that are usually observed in plots of acoustic velocities or elastic moduli vs. temperature (Figs. 5—10), are probably related to the effect of chemical reactions (loss of water, decomposition of light hydrocarbon ends, etc.) in the shale matrix. Similar effects have

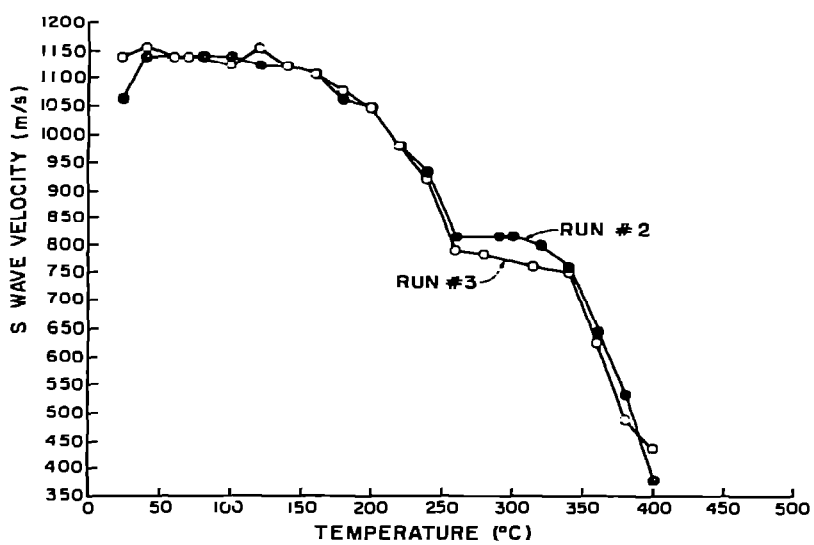

Fig. 8. Dependence of S wave velocity on temperature for a Kentucky oil shale sample. Runs 1 and 2 represent duplicate measurements.

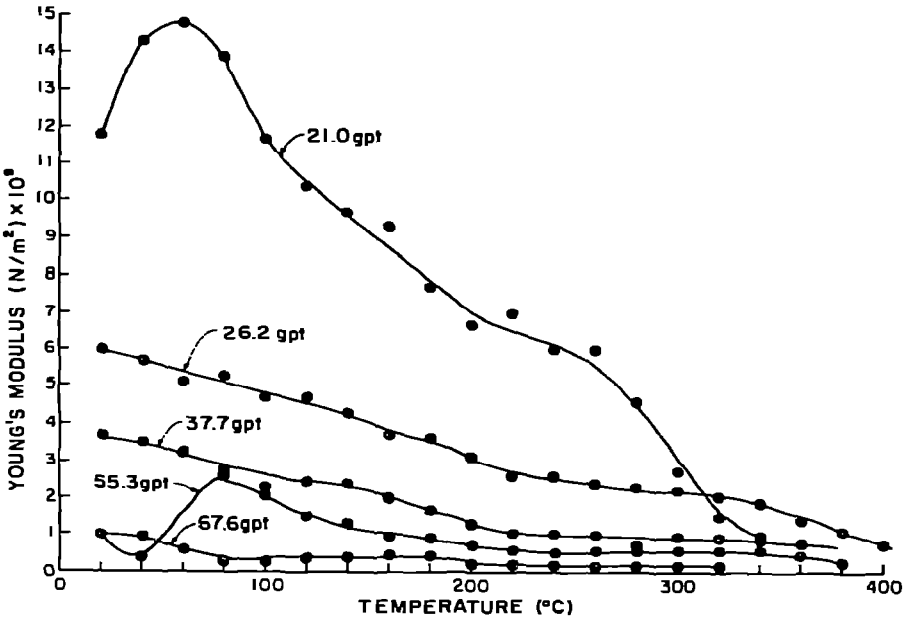

Fig. 9. Variation of Young's modulus with temperature and shale grade for Green River oil shales.

also been observed in the electrical [26] and thermal (e.g., specific heat) [27] behavior of these materials as a function of temperature. It is pertinent to note that these effects are seen at temperatures well below the range (450–500°C) at which thermal decomposition of oil shale kerogen is known to occur [28]. For example, a DSC or TG scan on Green River oil shale shows no anomalous thermal effects below ~450°C [26]. On the other hand, as seen above, the acoustic probe is much more sensitive to processes that are not

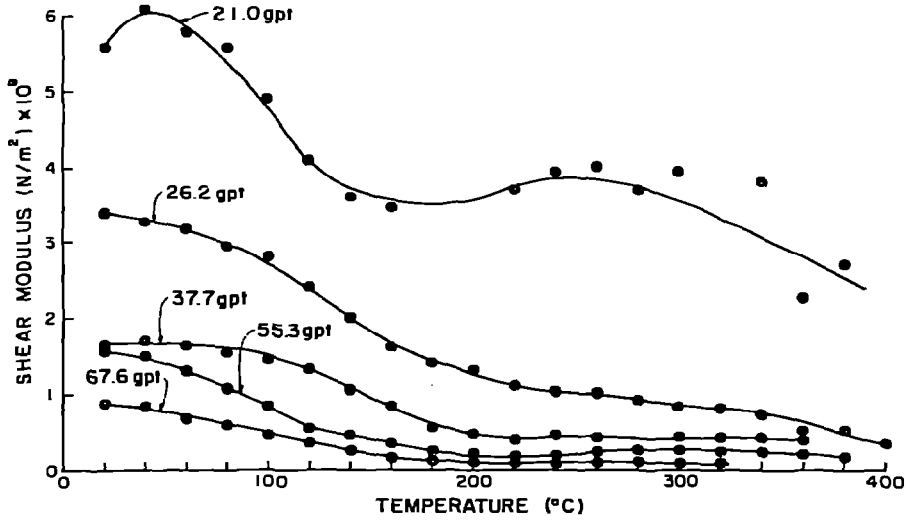

Fig. 10. Variation of shear modulus with temperature and shale grade for Green River oil shales.

reflected in a DSC or TG scan of the material. This sensitivity is characteristic of all Group B techniques discussed above. In this regard, the results shown in Figs. 5—10 serve to illustrate the use of the thermoacoustimetric technique as a viable thermoanalytical tool in its own right. The information that is gained from this technique on the thermomechanical behavior of the test specimen would be fully complementary to the data obtained from DSC or TG.

ACKNOWLEDGEMENTS

The authors wish to thank the U.S. Department of Energy and Laramie Energy Technology Center, Wyoming, for financial support of this research program. Thanks are also due to V.R. Pai Verneker for stimulating discussions and to R. Rosenvold and S. Biglari for enthusiastic help in sample preparation. Significant contributions from Chapman Young and Christopher Petit in the early stages of this research program are also gratefully acknowledged.

REFERENCES

1 K. Rajeshwar, R. Nottenburg, M. Freeman and J. DuBow, Thermochim. Acta, 33 (1979) 157.
2 R. Nottenburg, K. Rajeshwar, M. Freeman and J. DuBow, Anal. Chem., 51 (1978) 1149.
3 K. Lónvik, in I. Buzas (Ed.), Proc. 4th International Conference on Thermal Analysis, Heyden, London, 1975, p. 1089.
4 W.W. Wendlandt, 9th NATAS Conference, Chicago, Illinois, 23—26 September 1979.
5 D. Dollimore (Ed.), Proc. 1st European Symposium on Thermal Analysis, Heyden, London, 1976, pp. 31—35.
6 J.P. Redfern, in R.C. Mackenzie (Ed.), Differential Thermal Analysis, Vol. 1. Academic Press, London, 1970, Chap. 5, p. 123.
7 W.D. Emmerich and E. Kaisersberger, in H. Chihara (Ed.), Proc. 5th International Conference on Thermal Analysis, Heyden, London, 1977, p. 67.
8 P.K. Chatterjee, in I. Buzas (Ed.), Proc. 4th International Conference on Thermal Analysis, Heyden, London, 1975, p. 835.
9 R.C. MacKenzie, in H. Chihara (Ed.), Proc. 5th International Conference on Thermal Analysis, Heyden, London, 1977, p. 559.
10 L. Peselnick and R.M. Stewart, J. Geophys. Res., 80 (1975) 3765.
11 N.I. Christensen, J. Geophys. Res., 71 (1966) 3549.
12 P. Mattaboni and E. Schreiber, J. Geophys. Res., 72 (1967) 5160.
13 R.E. Thill and T.R. Bur, Geophysics, 34 (1969) 101; and refs. therein.
14 J.C. Jamieson and H. Hoskins, Geophysics, 27 (1963) 87.
15 G. Simmons, Proc. IEEE, 53 (1965) 1337.
16 O.L. Anderson and R. Liebermann, VESIAC State-of-the-Art Rep. No. 7885-4-X, Geophysics Laboratory, University of Michigan, Ann Arbor, 1966.
17 E. Schreiber, O.L. Anderson and N. Soga, Elastic Constants and Their Measurement, McGraw-Hill, New York, 1973, pp. 35—81.
18 E.P. Papadakis, J. Acoust. Soc. Am., 52 (1972) 843.
19 R.J. Blume, Rev. Sci. Instrum., 34 (1963) 1400.
20 A.M. Warner, M. Onoe and G.A. Coquin, J. Acoust. Soc. Am., 42 (1968) 1223.
21 C. Young and C. Petit, private communication, 1977.

22 H. Kolsky, Stress Waves in Solids, Dover Publication Inc., New York, 1963.
23 M.S. King and I. Fatt, Geophysics, 27 (1962) 590.
24 K. Rajeshwar, R. Nottenburg, J. DuBow and R. Rosenvold, Thermochim. Acta, 27 (1978) 357.
25 R. Nottenburg, K. Rajeshwar, R. Rosenvold and J. DuBow, Fuel, 57 (1978) 789.
26 R. Nottenburg, K. Rajeshwar, M. Freeman and J. DuBow, J. Solid State Chem., 28 (1979) 195.
27 D.B. Jones, K. Rajeshwar and J. DuBow, Ind. Eng. Chem., Prod. Res. Dev., in press.
28 K. Rajeshwar, R. Nottenburg and J. DuBow, J. Mater. Sci., 14 (1979) 2025.